Mesoscopic Correlations in Aqueous Alkylamine Mixtures Between Molecular and Micro Emulsions

Aurélien Perera *

November 12, 2025

Laboratoire de Physique Théorique de la Matière Condensée (UMR CNRS 7600), Sorbonne Université, 4 Place Jussieu, F75252, Paris cedex 05, France.

Abstract

Understanding how molecular correlations give rise to mesoscale organization is central to the physics of complex fluids such as hydrogen-bonded mixtures. In this work, we develop a mesoscale bridge formalism that connects the site–site Ornstein–Zernike (SSOZ) framework to the field theoretical Teubner-Strey (TS) approach. This bridge highlights how local orientational correlations, typically lost in the SSOZ closure, reemerge as effective long-range components at the mesoscale. The resulting theory provides a unified description of density fluctuations spanning molecular to mesoscopic length scales. The approach is illustrated using X-ray scattering spectra from simulated and experimental hydrogen-bonded fluids, showing that the TS representation captures the essential features of the mesoscale structure. Beyond this specific application, the proposed formalism offers a general route to interpret the structural crossover between microscopic interactions and collective mesoscale organization in complex fluids, including aqueous and amphiphilic systems.

1 Introduction

Liquids can be broadly classified into two main categories, separated by a wide conceptual "interface": simple liquids¹ and organized liquids.² Typical examples of the first class include for instance liquid nitrogen, benzene, or weakly polar cesium sulfide, where interactions remain essentially isotropic and short-ranged.³ The second class encompasses soft-matter and biological liquids, characterized by complex molecular architectures maintained by hard covalent bonds and soft bonds such as hydrogen bonds.

^{*}aup@lptmc.jussieu.fr

In between these two classes, molecular emulsions^{4,5} are characterized by partial microscopic segregation, leading to transient, nanoscale domains stabilized by molecular association through hydrogen bonding and/or hydrophobic effects. Because these systems combine structural disorder with local organization, one may introduce it as a third broad category of liquids, represented by water and aqueous mixtures. Despite the extensive literature devoted to each of these three families, there has been little theoretical effort to unify them under a single conceptual framework. Herein, this unification is attempted, guided by fundamental ideas from statistical physics. This approach is illustrated using aqueous alkylamine mixtures as model systems, since they naturally encompass all three categories within a single family.

This ambition echoes two historical viewpoints. The physicist Lev Landau, as cited by de Gennes, 6 regarded the theories of liquids as "neither convincing nor useful" in contrast with that of gases and solids—a challenge that de Gennes later addressed in his pioneering work on soft matter.² On the other hand, Rowlinson and Swinton⁷ famously remarked that aqueous mixtures of non-electrolytes would probably be the last liquids to be fully understood. These complementary perspectives—from a theoretical physicist, a soft-matter pioneer, and two chemists—motivate the search for a unifying view of the liquid state, encompassing simple disorder with organized disorder. They are also a good starting point to understand why microscopic liquid state theories are unable to reach beyond simple liquids, while field theories are not meant to the study of small molecules in solution. Molecular emulsions, such as aqueous amine mixtures are the strategic meeting place where both approches fail. Our hypothesis is that such systems encompass both large scale fluctuations and organized structures, while still remaining on the side of molecular liquids. In that, they require consistent theories of fluctuations, while staying close to the molecular level.

The key physical concept borrowed from fundamental theory is the competition between fluctuations and stability, which underlies the physics of critical phenomena. In such theories, fluctuations—particularly in density or concentration—are associated with k=0 modes, and the divergence of the corresponding response function signals proximity to a critical point. Some liquids, such as unoriented nematics, cannot be reduced to a single state point but rather form a continuum of critical states exhibiting permanent critical opalescence, but which are outside the scope of our present concern. Below this context is examined for aqueous alkylamines as opposed to aqueous alcohols.

In binary mixtures, phase separation typically follows a binodal with an upper critical solution temperature (UCST). At high temperature, miscibility is ensured by thermal disorder, while at lower temperatures the antagonistic interactions between unlike species dominate, leading to demixing. This is the case for aqueous alcohols, which demix beyond 1-propanol. The antagonism arises between charged polar groups (water and hydroxyl) and neutral alkyl groups, whose influence grows with increasing chain length and eventually overcomes the Coulomb affinity between the polar sites. Conversely, systems exhibiting a lower critical solution temperature (LCST) display the opposite behavior: they

demix at high temperature but remix upon cooling. Classical examples include aqueous mixtures of poly(N-isopropylacrylamide) (PNIPAM), poly(ethylene oxide) (PEO), and tertiary butanol, among others. Aqueous alkylamines belong to this latter category, showing a clear LCST beyond hexylamine—that is, for sufficiently long alkyl chains. One may then ask what microscopic mechanism allows the Coulomb association between water and the amine headgroup to promote remixing at lower temperature, despite the reduced thermal agitation. Walker and Vause⁹ proposed such a scenario within a renormalization group theory (RGT) framework, where tight solute—solvent dimer formation drives the LCST. In their picture, the homogeneous liquid corresponds to a dense fluid of such dimers.

Our results ^{10,11} confirm this scenario only partially. The formation of water—amine dimers through N–H···O hydrogen bonds is indeed observed, but the resulting liquid is not homogeneous. Instead, it is micro-heterogeneous, consisting of water nano-domains whose surfaces are saturated by amine nitrogen atoms. In other words, aqueous amines do not form a uniform liquid of dimers, but a disordered network of interfacial domains—an aspect entirely missed by the WV approach. This shortcoming of a very successful and leading fundamental theory can be interpreted as a need of a more microscopic approach which accounts for the observed features.

The alternative paradigm proposed herein is the formation of nano-domains, conceptually similar to the structure of micro-emulsions. The question examined here is if this picture is compatible with the Teubner–Strey (TS) model of modulated phases, 12 which describes the shift of the instability from k=0 to a finite $k\neq 0$. Such a transfer is typically associated with mesocopic/macroscopic ordering, as observed for micelle formation, lamellar or other layered phases. 13 In the case of aqueous amines, the observed structure corresponds instead to a disordered melt of broken layers—reorganized water and alkyl nano-domains forming what we have previously call a domain-ordered liquid. 5 At low amine concentrations, when there are insufficient amine—water dimers to stabilize extended water regions, macroscopic phase separation occurs, consistent with the LCST behavior. As the amine concentration increases, the water domains shrink and their surfaces become saturated with amine headgroups. The domains then decrease in size until, at high amine content, the system becomes a continuous amine phase embedding small water clusters.

The next section examines how the Teubner-Strey theory emerges from a field theorectic approach and underline the steps which are recovered in the third section where a more microscopic approach is developed, specifically introduce the conjecture on the meso-ranged bridge in order to reconcile both approaches. In the fourth section illustrates this progression using aqueous hexylamine and octylamine mixtures, highlighting the correspondence with the Teubner-Strey description inferred from molecular dynamics simulations. The last two sections gather remarks about the developments presented herein, and the final conclusion.

2 The Teubner–Strey behaviour of aqueous octylamine mixtures

In their seminal 1987 paper, Teubner and Strey derived a compact expression for the small- angle scattering intensity starting from a classical Landau-type free energy with a local order parameter ψ :

$$\beta F_{\rm FT}[\psi] = \int_{\Lambda} f(\psi, \nabla \psi, \Delta \psi) \, d\mathbf{r},\tag{1}$$

where $\beta = 1/k_BT$ and the subscript FT stands for "field theory." The free-energy density f is generally written in the Landau–de Gennes form, including powers of ψ and its spatial derivatives:

$$f = \sum_{n=0} a_n \psi^n + \sum_{n=1} c_n (\nabla^{2n} \psi).$$
 (2)

An important aspect of this formulation is the short-distance cutoff parameter Λ , which indicates that both the integrand and the resulting free energy are valid only for distances larger than Λ (in lattice theories, Λ would correspond to the lattice spacing). This cutoff acknowledges that the microscopic physics below Λ is not described by the model. In quantum field theory, for instance, this missing physics concerns the structure of the vacuum, for which no explicit theory exists. Approaching the $\Lambda \to 0$ limit leads to the well-known ultraviolet divergences, usually handled through renormalization procedures—an indirect way to bypass the unknown short-range physics. In classical, off-lattice field theories, Λ is often formally set to zero, and the analysis focuses instead on the large-r (infrared) or small-k limit, as in the renormalization group treatment of critical points. ¹⁴ Depending on the values and signs of the coefficients a_n and c_n , several scenarios arise for classical criticality, such as the Ornstein-Zernike (OZ) form, ¹⁵ Cahn–Hilliard spinodal decomposition, ¹⁶ Lifshitz points, and other modulated phases.¹⁷ A particularly relevant case is defined by $a_n = 0$ except for $a_2 > 0$, $c_1 < 0$, and $c_2 > 0$, which describes the characteristic features of micro-emulsions, i.e., systems with a negative "microscopic" surface tension. Under these conditions, the free energy reduces to:

$$\beta F_{\rm FT} = \int \left[a_2 \psi^2 + c_1 (\nabla \psi)^2 + c_2 (\Delta \psi)^2 \right] d\mathbf{r}. \tag{3}$$

The usual approach consists in expanding $F_{\rm FT}$ around the equilibrium mean value $\bar{\psi}$ by setting $\psi = \bar{\psi} + \delta \psi$ and truncating the expansion at quadratic order:

$$\beta F_{\rm FT}[\psi] = \beta F_{\rm FT}[\bar{\psi}] + \frac{1}{2} \int d\mathbf{r} \int d\mathbf{r}' \, \delta\psi(\mathbf{r}) \Gamma(|\mathbf{r} - \mathbf{r}'|) \delta\psi(\mathbf{r}'), \tag{4}$$

where the linear term vanishes by virtue of the equilibrium condition

$$\frac{\delta \beta F_{\rm FT}[\psi]}{\delta \psi(1)}\Big|_{eq} = 0,$$

and the kernel $\Gamma(|\mathbf{r} - \mathbf{r}'|)$ is the second functional derivative of the free energy,

$$\Gamma(|\mathbf{r} - \mathbf{r}'|) = \frac{\delta^2 \beta F_{\text{FT}}[\psi]}{\delta \psi(\mathbf{r}) \, \delta \psi(\mathbf{r}')} \Big|_{eq}.$$
 (5)

The generating functional for zero external field is the partition function,

$$Z = \int D\psi \, \exp[-\beta F_{\rm FT}[\psi]] \sim \int D\psi \, \exp\left[-\frac{1}{2} \int d\mathbf{r} \int d\mathbf{r}' \, \delta\psi(\mathbf{r}) \Gamma(|\mathbf{r} - \mathbf{r}'|) \delta\psi(\mathbf{r}')\right],$$
(6)

which is a continuous Gaussian functional integral. In Fourier space this becomes:

$$Z \sim \int d\psi \exp \left[-\frac{1}{2} \int d\mathbf{k} \int d\mathbf{k}' \, \delta\psi(\mathbf{k}) \Gamma(|\mathbf{k} + \mathbf{k}'|) \delta\psi(-\mathbf{k}') \right], \tag{7}$$

where the kernel is readily obtained from Eq. (3) as

$$\Gamma(k) = a_2 + c_1 k^2 + c_2 k^4. \tag{8}$$

The scattering intensity I(k) is proportional to the structure factor $S(k) = \langle \psi(\mathbf{k})\psi(-\mathbf{k})\rangle$, which in the Gaussian approximation is simply the variance of the fluctuations:

$$\langle \psi(\mathbf{k})\psi(-\mathbf{k})\rangle \propto \Gamma^{-1}(k).$$

This definition leads directly to the Teubner–Strey (TS) expression:

$$I(k) \propto \frac{A}{a_2 + c_1 k^2 + c_2 k^4},$$
 (9)

where A is a normalization constant. The TS form contrasts with the Ornstein–Zernike limit, which corresponds to $c_1 > 0$ and $c_2 = 0$. In the following sections, this formalism will be rederived from a more microscopic approach. Teubner and Strey demonstrated that Eq. (9) successfully reproduces small-angle neutron scattering (SANS) data for a variety of micro-emulsions, such as D_2O –decane–36/58 AOT droplet systems. ¹² Equation (9) also implies a corresponding real-space correlation function of the form:

$$I(r) = \bar{d} \frac{\exp(-r/\xi)}{r} \sin(\frac{r}{\bar{d}}), \qquad (10)$$

where the oscillation period is governed by the characteristic domain size $d=2\pi \bar{d}$, and the correlation length ξ and domain spacing d are related to the parameters in Eq. (9) by:¹²

$$d = 2\pi \left[\frac{1}{2} \sqrt{\frac{a_2}{c_2}} - \frac{1}{4} \frac{c_1}{c_2} \right],\tag{11}$$

$$\xi = \left[\frac{1}{2} \sqrt{\frac{a_2}{c_2}} + \frac{1}{4} \frac{c_1}{c_2} \right]. \tag{12}$$

The correlations represented by I(r) therefore decay exponentially with correlation length ξ , as in the Ornstein–Zernike case,¹ but include an additional oscillatory term whose period is determined by the domain size d.

To connect this mesoscopic description with a microscopic one, one can relate the real-space correlations to the atom-atom pair correlation functions $g_{ij}(r)$ through the total atom- atom structure factors $S_{ij}(k)$ using the Debye relation:^{18,19}

$$I(k) = r_0^2 \rho \sum_{ij} f_i(k) f_j(k) S_{ij}(k),$$
(13)

where $\rho = N/V$ is the molecular number density, $f_i(k)$ are the atomic form factors, and $r_0 = 2.8179 \times 10^{-13}$ cm is the classical electron radius. The total structure factor $S_{ij}(k)$ is defined as:²⁰

$$S_{ij}(k) = w_{ij}(k) + \rho H_{ij}(k), \tag{14}$$

where $w_{ij}(k)$ is the intra-molecular structure factor and $H_{ij}(k)$ is related to the Fourier transform of the intermolecular pair correlation function:

$$H_{ij}(k) = \int d\mathbf{r} \left[g_{ij}(r) - 1 \right] e^{i\mathbf{k} \cdot \mathbf{r}}.$$
 (15)

The purpose of the section is to reconcile Eqs. (9) and (13) by showing that the former can be derived from the latter in the small-k limit, and to illustrate the physical relevance of this correspondence for aqueous alkylamine mixtures.

3 Liquid-state statistical theory basis for TS behaviour

Soft-matter systems are often described by field-theoretic, mesoscopic approaches in which some atomic details (e.g., explicit solvent degrees of freedom) are coarse-grained.^{21,22} At the opposite end, molecular liquids admit a fully microscopic statistical description.²³ A key ingredient of the field-theoretic route is a coarse-grained order parameter (a random field) from which mesoscopic correlation functions and structure factors—such as Eq. (9)—are built. Liquid-state theory also relies on random variables, but at the microscopic level: the site (atom) density

$$\rho_{i_a}(\mathbf{r}) \equiv \sum_{n \in i_a} \delta(\mathbf{r} - \mathbf{r}_n), \qquad (16)$$

where i_a labels site i on species a (e.g. $i = O_W$ and $a = H_2O$, or i = N for a = amine), and the sum runs over all atoms of type i_a . From these microscopic variables, one constructs various correlation functions, and in particular the microscopic pair correlation functions $g_{i_aj_b}(r)$. Our aim is to relate the mesoscopic and microscopic descriptions on a single, controlled footing. Aqueous alkylamines provide an ideal testbed, because the relevant length scales

(molecular vs. domain) are both experimentally accessible and well-separated but coupled.

Theoretical developments below show how the two routes connect. The approach departs from the standard literature by identifying the *bridge function* as the natural carrier of mesoscopic (domain-scale) oscillations.

3.1 Statistical theory of molecular emulsions

Consider molecular liquids as atomistic fluids in which molecular connectivity acts as a constraint. Each site is labeled by the composite index i_a , with a the species index (water, amine, ...) and i the site identity within that species (O, H, N, C_1 , ...). The site–site pair distribution satisfies the exact Morita–Hiroike relation

$$g_{i_a j_b}(r) = \exp\left[-\beta v_{i_a j_b}(r) + h_{i_a j_b}(r) - c_{i_a j_b}(r) + b_{i_a j_b}(r)\right],$$
 (17)

where $v_{i_aj_b}(r)$ is the pair potential between sites i_a and j_b at distance r, $h_{i_aj_b}(r) = g_{i_aj_b}(r) - 1$, $c_{i_aj_b}(r)$ is the direct correlation function, and $b_{i_aj_b}(r)$ is the bridge function. The latter is an infinite series over higher-order direct correlation functions,

$$b_{i_{a}j_{b}}(r) = \sum_{n\geq 2} \frac{1}{n!} \sum_{\{\ell_{c_{k}}^{(k)}\}_{k=3}^{n+1}} \prod_{k=3}^{n+1} \rho_{\ell_{c_{k}}^{(k)}} \int \prod_{k=3}^{n+1} d\mathbf{r}_{k} \left[\prod_{k=3}^{n+1} h_{i_{a}\ell_{c_{k}}^{(k)}}(r_{1k}) \right] c_{\{\ell_{c_{k}}^{(k)}\}j_{b}}^{(n+1)}(\mathbf{r}_{13}, \dots, \mathbf{r}_{1 n+1}),$$

$$(18)$$

where $c^{(n+1)}$ denotes the (n+1)-body direct correlation function and the set $\{\ell_{c_k}^{(k)}\}$ runs over n-1 intermediate sites. To illustrate this expression with rather heavy indexing conventions, the explicit expression for the first term is given:

$$b_{i_a j_b}(r) = \sum_{l_c, m_d} \frac{\rho_{l_c} \rho_{m_d}}{2!} \int d\mathbf{r}_3 \int d\mathbf{r}_4 h_{i_a l_c}(r_{13}) h_{i_a m_d}(r_{13}) c_{l_c m_d j_b}^{(3)}(r_{13}, r_{23})$$

From the presence of all order direct correlations, it is evident that solving Eq. (18) exactly is intractable, and even the convergence of the series is subtle (lack of convergence is known in 1D;²⁴ indications exist of delicate behavior in 3D.²⁵ This motivates an alternative route guided by asymptotics and physical separation of length scales.

In the large-r limit, expanding the exponential in Eq. (17) to first order yields an exact asymptotic relation for the direct correlation function:

$$c_{i_a j_b}(r \to \infty) = -\beta v_{i_a j_b}(r) + b_{i_a j_b}(r).$$
 (19)

This is a key identity, which emphasizes a point often overlooked: while $b_{i_aj_b}(r)$ is usually assumed shorter-ranged than dispersion forces (and therefore neglected in HNC-like closures), complex liquids with self-assembly at multiple

scales (soft and biological matter) generally require a *mesoscopic*, long-distance contribution in $b_{i_a j_b}(r)$ to encode domain order.

The direct correlation is therefore decomposed as

$$c_{i_a j_b}(r) = c_{i_a j_b}^{(R)}(r) + b_{i_a j_b}^{(SR)}(r) + b_{i_a j_b}^{(MR)}(r),$$
 (20)

where $c^{(R)}$ is a reference (short-ranged) contribution (e.g. from an integral-equation closure), $b^{(SR)}$ is a short-ranged bridge correction (often tuned to match thermodynamic targets such as internal energy or compressibility), and $b^{(MR)}$ captures the essential mesoscopic contribution responsible for domain-scale correlations:

$$b_{i_a j_b}^{(MR)}(r \to \infty) = b_{i_a j_b}(r).$$
 (21)

Next, weak microscopic inhomogeneities around a uniform state are considered, with local densities given by Eq. (16) and

$$\delta \rho_{i_a}(\mathbf{r}) \equiv \rho_{i_a}(\mathbf{r}) - \rho_{i_a}. \tag{22}$$

The *total* direct correlation functions are generated by functional derivatives of the Helmholtz free-energy with respect to the site densities:

$$C_{\{j_b:n\}}^{(n)}(\mathbf{r}_1,\dots,\mathbf{r}_n) = \frac{\delta^{(n)}\beta F[\{\rho_{i_a}\}]}{\prod_{\{j_b:n\}}\prod_{m=1}^n \delta\rho_{j_b}(\mathbf{r}_m)}.$$
 (23)

Expanding $F[\{\rho_{i_a}\}]$ around the homogeneous equilibrium (βF_0) yields

$$\beta F[\{\rho_{i_a}\}] = \beta F_0 + \int d1 \sum_{i_a} \frac{\delta \beta F[\{\rho_{\alpha}\}]}{\delta \rho_{i_a}(1)} \bigg|_{0} \delta \rho_{i_a}(1) + \frac{1}{2} \int d1 \int d2 \sum_{i_a, j_b} \frac{\delta^2 \beta F[\{\rho_{i_a}\}]}{\delta \rho_{i_a}(1) \delta \rho_{j_b}(2)} \bigg|_{0} \delta \rho_{i_a}(1) \delta \rho_{j_b}(2) + \dots, \quad (24)$$

where derivatives are evaluated at uniform densities (subscript 0). The linear term vanishes by equilibrium:

$$\frac{\delta\beta F[\{\rho_{\alpha}\}]}{\delta\rho_{i_{a}}(1)}\bigg|_{0} = 0. \tag{25}$$

Recognizing the second functional derivative as the total direct correlation function $C_{i_aj_b}(\mathbf{r}_1,\mathbf{r}_2)$ and truncating at quadratic order leads to

$$\beta F[\{\rho_{i_a}\}] = \beta F_0 - \frac{1}{2} \int d\mathbf{r} \int d\mathbf{r}' \, \boldsymbol{\delta} \boldsymbol{\rho}(\mathbf{r}) \, \mathbf{C}(|\mathbf{r} - \mathbf{r}'|) \, \boldsymbol{\delta} \boldsymbol{\rho}(\mathbf{r}'), \qquad (26)$$

where $\delta \rho(\mathbf{r})$ collects all site-density deviations and \mathbf{C} is the matrix of total site-site direct correlation functions. This expression mirrors the field-theory quadratic form in Eq. (4), but here it is derived *microscopically*.

The matrix elements can be written as

$$C_{i_a j_b}(|\mathbf{r} - \mathbf{r}'|) = \sqrt{\rho_{i_a} \rho_{j_b}} \left[V_{i_a j_b}(|\mathbf{r} - \mathbf{r}'|) - \sqrt{\rho_{i_a} \rho_{j_b}} c_{i_a j_b}(|\mathbf{r} - \mathbf{r}'|) \right], \tag{27}$$

where V can be identified (approximately) with the inverse of the intramolecular correlation matrix W of RISM, $V \approx W^{-1}$.

Using the decomposition in Eq. (20), the short-range (reference + short-range bridge) and mesoscopic bridge contributions are separated:

$$C_{i_a j_b}(r) = C_{i_a j_b}^{(V)}(r) + \rho_{i_a} \rho_{j_b} b_{i_a j_b}^{(MR)}(r),$$

with

$$\mathcal{C}_{i_aj_b}^{(V)}(r) = \sqrt{\rho_{i_a}\rho_{j_b}} \left[V_{i_aj_b}(r) - \sqrt{\rho_{i_a}\rho_{j_b}} \left(c_{i_aj_b}^{(R)}(r) + b_{i_aj_b}^{(SR)}(r) \right) \right]. \label{eq:constraint}$$

Transforming Eq. (26) to Fourier space,

$$\beta F[\{\rho_{i_a}\}] = \beta F_0 - \frac{1}{2(2\pi)^3} \int d\mathbf{k} \int d\mathbf{k}' \, \delta \boldsymbol{\rho}(\mathbf{k}) \, \mathbf{C}^{(V)}(|\mathbf{k} + \mathbf{k}'|) \, \delta \boldsymbol{\rho}(-\mathbf{k}')$$

$$- \frac{1}{2(2\pi)^3} \int d\mathbf{k} \int d\mathbf{k}' \, \delta \boldsymbol{\rho}(\mathbf{k}) \, \mathbf{B}^{(MR)}(|\mathbf{k} + \mathbf{k}'|) \, \delta \boldsymbol{\rho}(-\mathbf{k}'),$$
(28)

where the superscript "V" is stands for "vacuum": the first (short-range) contribution $\mathbf{C}^{(V)}$ plays the role of a background (or "vacuum") set by molecular details below the ultraviolet cutoff Λ , while the second term $\mathbf{B}^{(MR)}$ collects the mesoscopic bridge contributions responsible for domain-scale structure. In the field-theoretic analogy, $\mathbf{B}^{(MR)}$ is the microscopic origin of the kernel $\Gamma(k)$ in Eq. (4). Field theories entirely neglect the $\mathbf{C}^{(V)}$ contribution because the underlying physics is either neglected, such as in soft matter theories where small solvent and some solute molecules are ignored, or unknown such as in quantum field theories since the physics of the vacuum is unknown.

This correspondence provides a microscopic basis for the mesoscopic TS kernel and motivates the emergence of a finite-k instability from the site–site description. In the next sections, this conjecture is supported by analyzing correlation functions of aqueous alkylamine mixtures from molecular simulations ¹¹ together with X-ray scattering data. ¹⁰

4 Illustration with aqueous hexylamine mixtures

Detailed results from x-ray experiments and computer simulations have been reported in Refs. ^{10,11} Herein, aqueous hexylamine and aqueous octylamine mixtures are considered, with appropriate alkyl chain length to make these alkylamine act as surfactant-like molecules. It is not sufficient, however, that such molecules have a polar head and an sufficiently long alkyl tail in order to create micro-segregation. For instance, while octanol has a similar polar head/alkyl tail structure, aqueous octanol mixture are immiscible for a large range of solute concentration. The key to miscibility is that the polar head and water molecule "anchor" within each other. In the case of the amine head group, it is the two hydrogen which allow to "anchor" water, or water to "mingle" with the amine head groups. ²⁶ This is illustrated through the fact that computer

simulations of various models show segregated water domains to be surrounded by nitrogen atoms, which in turn stabilize these water nano-domains.

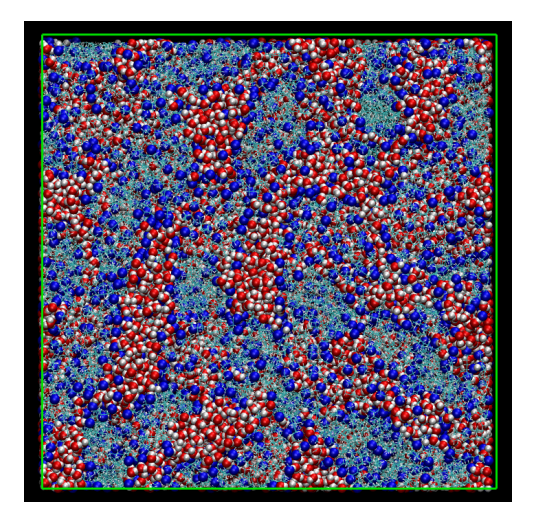


Figure 1: Snapshot of the 30% aqueous-hexylamine mixture illustrating the water domains surrounded by nitrogen atoms which delimitate them from the alkyl "bath".

This "anchoring"/"mingling" physics does not occur in the case of aqueous octanol for instance, which is the main reason why alkanols demix from water starting from butanol, while butylamine is fully miscible with water, and higher alkylamines mix above 20% solute content. For lower concentration, there is no sufficient amine head groups to stabilize the larger water nano-domains.

4.1 Teubner-Strey fitting of x-ray spectra

First, the fact that higher aqueous-alkylamine behave as micro-emulsions is demonstrated by fitting the x-ray scattering pre-peaks with the TS formula of Eq.(9).

Fig.2 shows how the scattering pre-peaks of aqueous hexylamine mixtures (blue curves) are nicely fitted by the TS formula (red curves), both for the experimental results (lower panels) and spectra computed from simulations (upper panels), and for various hexylamine mole fractions x. The values for the domain size d and the OZ correlation length ξ , as extracted from the fits according to Eqs.(11,12), are indicated in each panels. What is remarkable is that the small-k left part of the SPP is better fitted than the large-k side. This is because the TS fit is suited for small-k, and also because hexylamine is more of a large molecule than a true surfactant molecule, which is why the large-k side, closer to distances comparable to atom sizes, as described by the main peaks around $k_{MP} \approx 1.5 \mbox{Å}^{-1}$, which is roughly $r \approx 2\pi/k_{MP} \approx 4\mbox{Å}$. Interestingly, this is

more true of the simulation spectra than the experimental ones, which is probably a problem of the force field model and the ability to describe entirely the water-solute mingling processes.

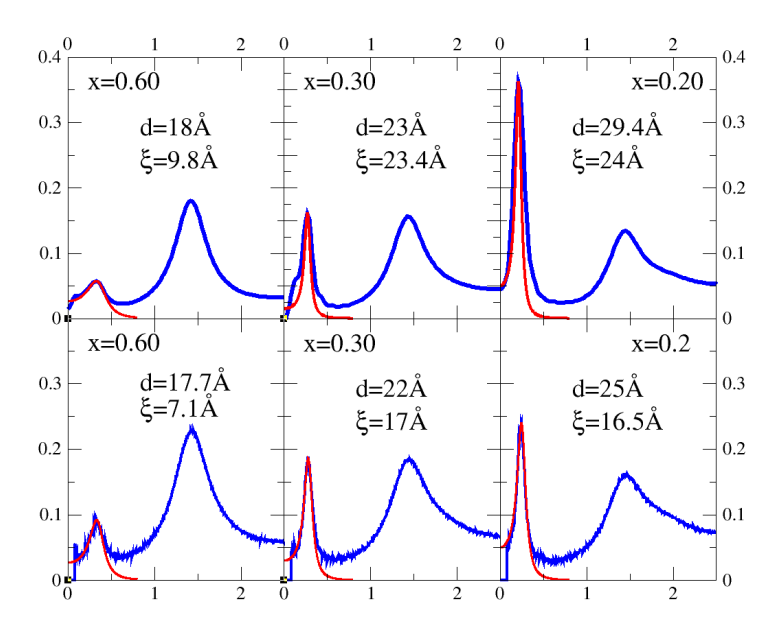


Figure 2: Illustration of the TS fitting of the scattering pre-peaks for aqueous-hexylamine, for various hexylamine mole fractions x shown in each panels. The x-ray spectra are shown in blue lines, and the TS fitting curves in red lines. The lower panels are for the experimental data¹⁰ and the upper panels for the simulation data.¹¹ The domain sizes d and OZ correlation lengths ξ are given in each panel.

It is also very interesting that the domain size parameter d from the fit is very close the distance corresponding to the pre-peak positions k_{PP} :

$$d \approx \frac{2\pi}{k_{PP}}$$

which confirms that both quantities are related.

It can be seen, however, that the domain sizes and correlation lengths are in overall good agreement between the experimental and calculated spectra. This agreement is excellent for large amine content, and the domain sizes are also in better overall agreement than the correlation lengths. This is because fluctuations are notoriously difficult to capture with force field models, as when computing phase boundaries.²⁷

A similar fitting has been conducted for aqueous octylamine, as illustrated in Fig.3. In this case, both the experimental and calculated spectra are well fitted from the small and large k sides. It indicates that octylamine might be closer to a surfactant, principally in view of the alkyl tail length.

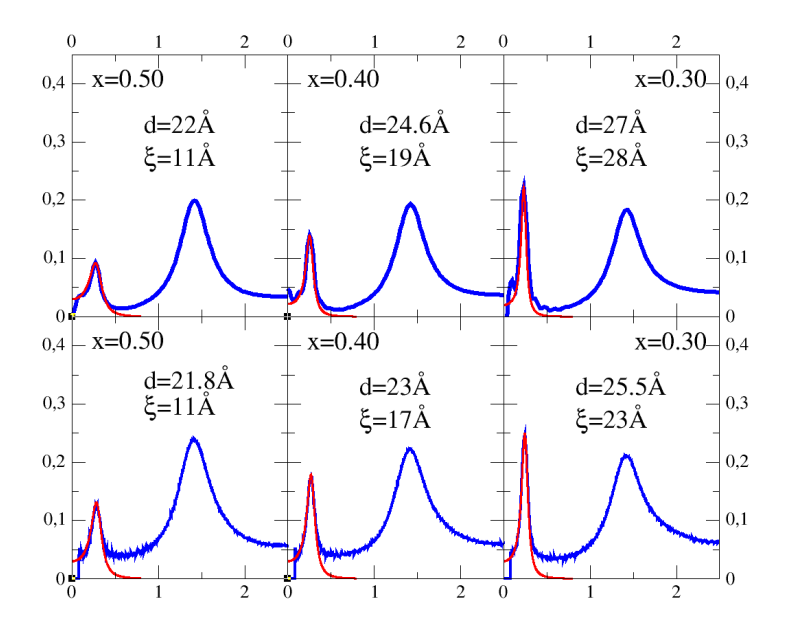


Figure 3: Illustration of the TS fitting of the scattering pre-peaks for aqueous-octylamine, for various hexylamine mole fractions x shown in each panels. The line and other details are as in Fig.2

The agreements for the d and ξ parameters are comparable to the case of hexylamine.

It can be seen that the domain size parameters and correlation lengths increase with increasing water content (decrease with amine mole fraction x) when the water nano-domain become larger. The alkyl size dependence is less clear. Furthermore, ξ increases faster than d when the water content is increased, which is consistent with the fact that ξ should diverge at the spinodal of the phase separation at small amine mole fractions.

4.2 Teubner-strey fitting of the tail of the correlation functions

In Ref.,¹¹ the large distance tails of the correlation functions were studied, and it was shown that these showed large scale oscillations which correspond with the mean segregated domain size. These were very small amplitude oscillations, whose full decay could not be observed within the simulation box sizes (around $L \approx 100 \mathring{A}$, corresponding to N=16000 molecules). An attempt to complement these oscillatory behaviour by using a functional form that is compatible with the k-space form of TS behaviour in Eq.(9) as well as with the related r-space

form Eq.(10), is accomplished with with the following expression.

$$\lim_{r \ge R_c} g_{ij}(r) = g_{ij}(R_c) \exp(-(r - R_c)/\xi) \sin(\frac{2\pi r}{d})$$
 (29)

where $R_c = L/2$ corresponds to half box length, until which the correlation functions are generally evaluated in computer simulations.

Fig.4 illustrates this TS extension fitting of the g(r) in the case of 20% aqueous-hexylamine mixtures. Three typical atom-atom correlation functions are selected, namely $g_{O_WO_W}(r)$, $g_{NO_w}(r)$ and $g_{NN}(r)$. The short range parts are shown in the main panel, where the atom-atom correlation with the typical atom-size oscillations can be seen. Just at the rim of the figure, for distances about $18-20\mathring{A}$, the start of the domain oscillations can be observed, the latter which are highlighted in the lower inset for distances up to $50\mathring{A}$, and correspond to half box length for this. Such domain oscillations can be captured only by allowing sufficiently large system sizes (herein N=16000 molecules have been used¹¹). If the system size was limited to N=2000 molecules, the half box size would only cover distances up to $20\mathring{A}$, which is barely sufficient to observe the first domain oscillation. Domain oscillation magnitudes are about one order of magnitude smaller than the atom-atom correlation oscillations.

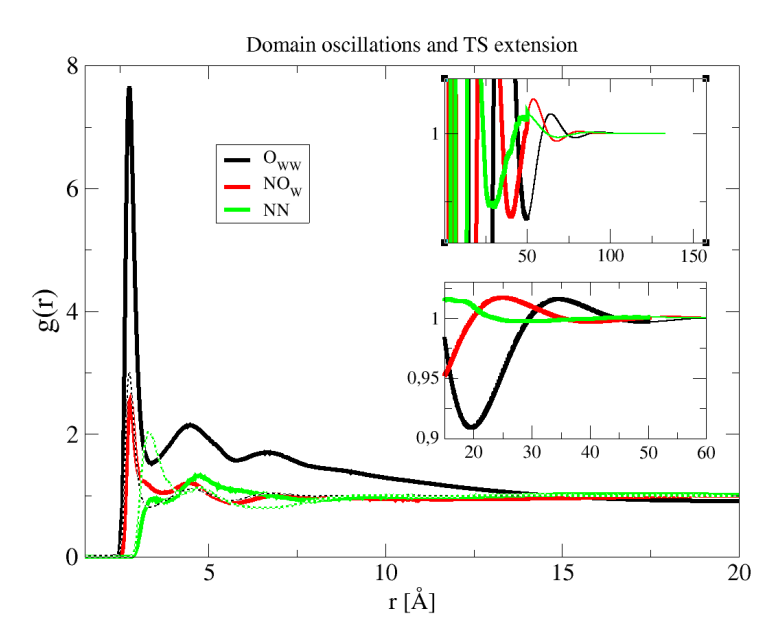


Figure 4: Typical atom-atom correlation functions for the 20% aqueous-hexylamine mixture, illustrating the short (main panel), medium (lower inset) and long/meso (upper inset) range behaviour. The neat liquid correlation functions are shown in dashed lines in the main panel (black for water and green for hexylamine). The thin lines in the upper inset are the TS fitting extension of Eq.(29).

The TS extension from Eq.(29) can be seen at the rim of this inset for r > 50Å. This extension is fully illustrated in the upper inset, where one observes how the fitting smoothly and naturally extends the domain oscillations above the half-box size for distances greater than 50Å. The parameters d and ξ are taken from the TS fits of the pre-peak behaviour in Fig.2. In the accompanying SI document, Fig.SI.1 shows the full range of the TS fitn and how the molecular range and field theoretic ranges can be separated out.

A similar fit for the case of 30% aqueous-octylamine is shown in Fig.5. In this case, the domain oscillations are more sustained, and the TS extension fit is better defined.

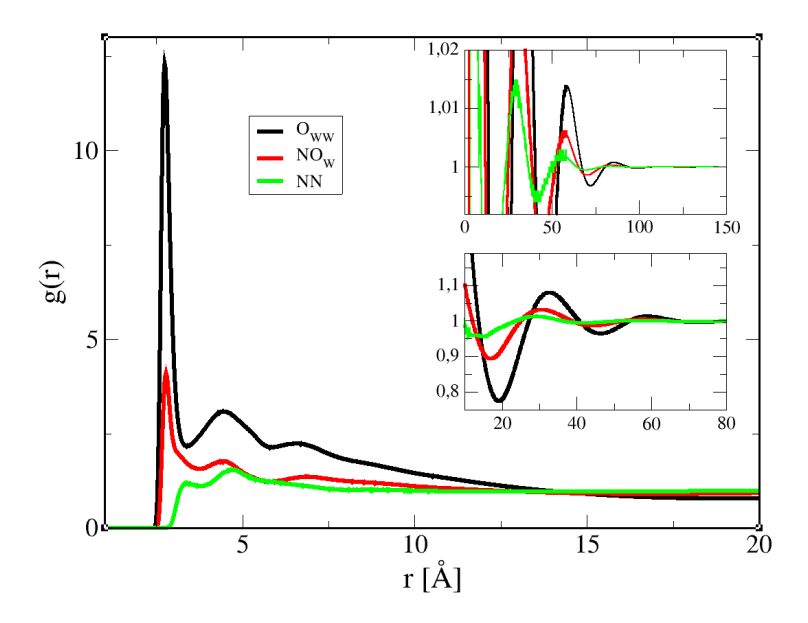


Figure 5: Typical atom-atom correlation functions for the 30% aqueous-octylamine mixture. The plot details are as in Fig.4

It is equally interesting to examine the structure factors corresponding to the g(r) shown in Figs.(4,5). In Fig.6 the atom-atom structure factors are shown for the case of 30% aqueous-octylamine, corresponding to the g(r) shown in Fig.5. The main panel shows a zoom over the pre-peaks parts. The original data is shown in thick curves, while those corresponding to the TS-extension are shown in thinner lines. It can be seen that, except for the very small k below $k \approx 0.2 \mathring{A}^{-1}$, the two curves exactly superpose, confirming that the TS-extension provides a better k=0 behaviour than the S(k) corresponding to the truncated g(r) of the original data. The original data is seen to generate small spurious oscillations, more visible in the inset.

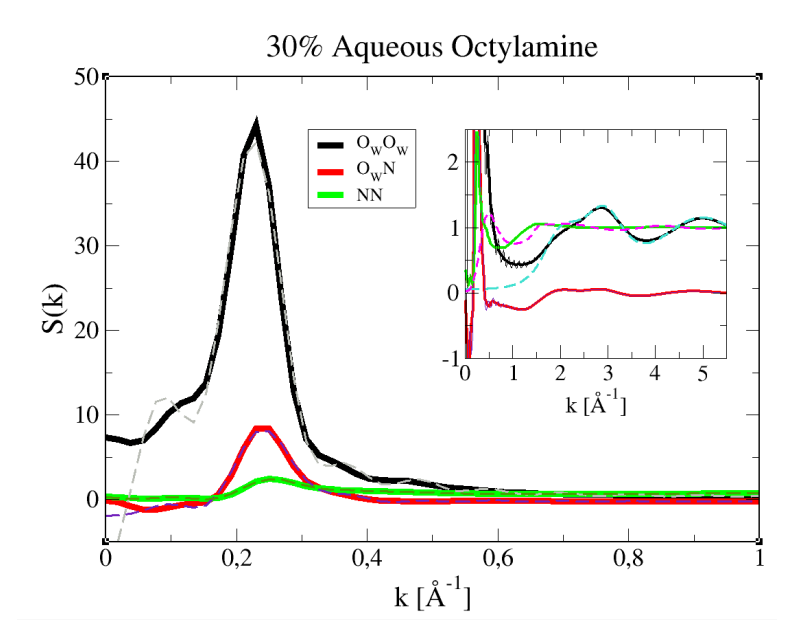


Figure 6: Typical atom-atom structure factors $S_{i_aj_B}(k)$ for the 30% aqueous-octylamine mixture. The main panel is a zoom over the pre-peak region, while the inset shows the main peak region. Thick curves show the S(k) from the original g(r) obtained from computer simulations. The thinner curves are the Fourier transforms of the TS-extended g(r) shown in Fig.5.

The inset shows the main peak region, together with the neat liquids S(k), shown in dashed cyan for water and magenta for octylamine. It is seen that the structure of the water domain is nearly identical to that of bulk water.

In order to better enforce the quality of the TS-extension, the running Kirkwood-Buff integrals (RKBI) defined by, ²⁸ ae shown in Fig.7

$$G_{i_a j_b}(r) = 4\pi \int_0^r ds s^2 \left[g_{i_a j_b}(r) - 1 \right]$$
 (30)

whose $r \to \infty$ limit are the Kirkwood-Buff integrals (KBI). Fig.7 demonstrates the smooth continuation of the domain oscillations towards well defined horizontal asymptotes which define the KBI.

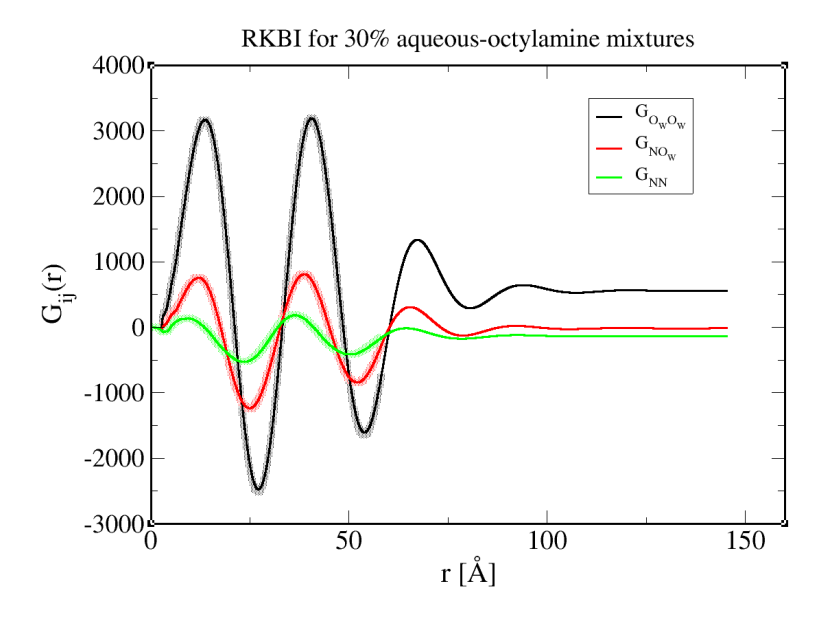


Figure 7: Running Kirkwoof-buff integrals for the 30% aqueous-octylamine mixtures. The thick lines represent RKBI of the g(r) from simulation data, and the thinner lines the RKBI from the TS-extended g(r).

It is obvious that such asymptotes cannot be obtained from the current simulations, since the corresponding data stops at $r\approx 60 \mathring{A}$, as indicated by the thick lines. In this region, the domain oscillations are still important and cannot help decide the KBI values. The TS-extension allows unambiguous determination of the KBI. It also confirms that separation between the inner range and meso-range correlations, which is conjectured in Section 3

Finally, in order to confirm that the TS extension does not alter the prediction of the scattering intensities, Fig.8 shows the x-ray spectra obtained from the original g(r) from the simulations and that obtained from the TS-extension of each of the atom-atom g(r). These are shown in dashed curves. It can be seen that the superposition of both curves in nearly exact, except from the small numerical artifacts from the Fourier transforms of the original g(r) which do not converge to 1 at the end of the half-box.

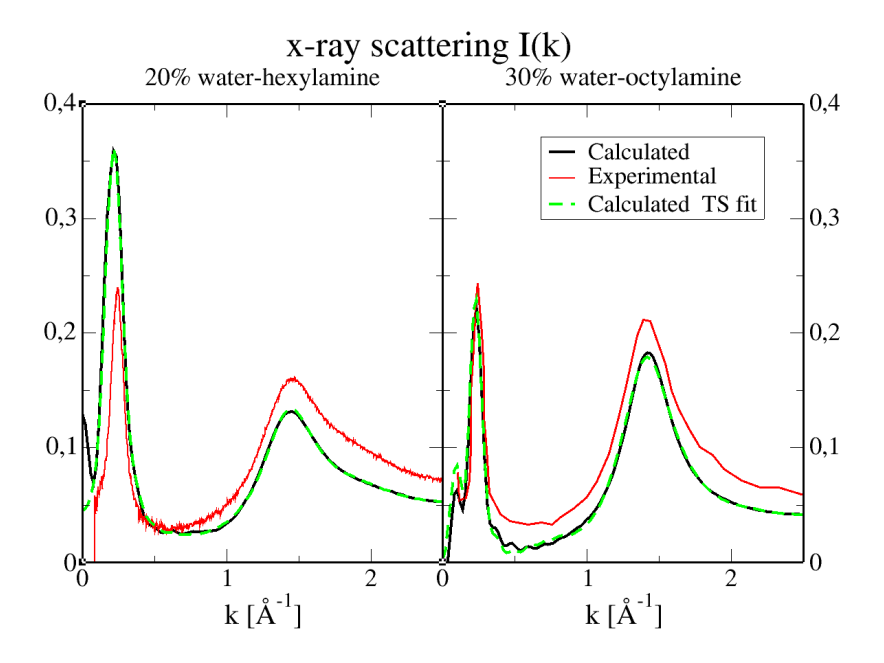


Figure 8: x-ray scattering intensities comparing the experimental data (red curves) to the calculated ones, one from the g(r) obtained from the simulations (black lines) and that from the TS-extended g(r) (dashed green lines). Left panel is for 20% aqueous hexylamine and right panel for 30% aqueous octylamine.

The figure equally shows the type of agreement with the experimental data one can obtain from model computer simulations, which was previously studied in Refs.^{10,11} The agreement tends to be better for the longer octylamine. This enforces the conjecture proposed in Section 3, since it shows that systems closer to the micro-emulsion are better described by model simulations, precisely because the meso-range structure decouples better from the small range atom/molecular range, which has been called herein called the "Vacuum" range.

The SI document shows how the TS expression, while describing perfectly the meso-physics under the pre-peak, cannot account for the molecular details. Fig.SI.2 shows how I(k) is the result of huge cancellations between the partial scattering intensities from water, octylamine and cross species contributions. Similarly, Fig.SI.3 illustrates the partial atom-astom structure factors contain all the molecular details, including those which contribute to the pre-peaks. These details can only be captured by a fully microscopic theory.

5 Discussion

The central hypothesis of this work—that the mesoscopic correlations of soft-matter systems originate from the meso-range component of the bridge function—is far from trivial. It challenges the long-standing view that the bridge function

is always shorter-ranged than the direct correlation function.²⁹ This belief is supported by studies of simple liquids, where b(r) has been extracted from simulations of Lennard–Jones^{30,31} or hard-sphere³² models. In those cases, as well as in self-consistent closures,³³ the bridge function indeed appears weak and rapidly decaying.

However, complex liquids displaying self-assembly or domain formation behave differently. Our conjecture is supported by the limited success of the hypernetted-chain (HNC) closure, which—though the most complete integral-equation theory—neglects the bridge function entirely.³⁴ We argue that it is precisely this neglect that prevents HNC from describing molecular emulsions and soft-matter systems properly: the missing higher-order terms embedded in the meso-range bridge function (Eq. 18) are essential to represent collective mesoscopic organization.

The apparent success of alternative closures such as Percus–Yevick (PY)¹, hybrid mean spherical approximation (HMSA)³⁵, or Kovalenko–Hirata (KH)³⁶ closures has, in retrospect, diverted attention from the fundamental limitations of HNC. The bridge function remains difficult to extract reliably from simulations,^{37,38} yet distinguishing between its short-range and mesoscopic parts clarifies its physical role. The short-range component governs local coordination, whereas the meso-range component controls domain-scale aggregation and self-assembly.

Even if short-range structural details remain imperfectly captured, incorporating an appropriate meso-range bridge term may allow HNC-type closures to reproduce soft-matter structure quantitatively. The Teubner–Strey form used here thus appears as a promising kernel for developing explicit mesoscopic bridge functionals that can be integrated within the framework of molecular integral-equation theory.

6 Conclusion

A theoretical framework has been proposed, which unifies molecular liquids and soft-matter systems such as micro-emulsions within a single statistical-mechanical description. The key conjecture is that the long-range structure of complex liquids originates from mesoscopic contributions of the bridge function—a hypothesis that departs from the established assumption of its purely short-ranged character in simple liquids.

Through the example of aqueous alkylamine mixtures, which exhibit persistent micro-heterogeneity, it was shown that domain-scale oscillations in the correlation functions stem from a Teubner–Strey–type kernel. This mesoscopic component decouples from the local, atomistic correlations and provides the microscopic foundation of the Landau–Ginzburg–de Gennes field theory used to describe modulated phases.

The resulting connection between molecular-scale statistical mechanics and mesoscopic field theories opens the way for integral-equation approaches to explore more complex soft-matter systems. Such a unified description offers a valuable theoretical complement to computer simulations, bridging the gap between microscopic interactions and emergent supramolecular organization.

Data availability

The data used in this work is available upon request to the author.

Supporting Information

The Supporting Information document contains information on the short coming of field theoretical approaches when it concern molecular details.

Acknowledgments

The author thanks Bernarda Lovrinčević, Martina Požar and Christian Sternemann for insightful comments.

This work was supported by the French-German collaborations PROCOPE (50951YA), Analysis of the molecular coherence in the self-assembly process: experiment and theory.

References

- ¹ Hansen, J.-P.; McDonald, I. *Theory of Simple Liquids*. Academic Press, Elsevier, Amsterdam, 3rd ed., **2006**.
- ² de Gennes, P. G. Soft matter. Rev. Mod. Phys. **1992**. 64, 645–648.
- ³ Trond S. Ingebrigtsen, T. B. S.; Dyre, J. C. What is a simple liquid? *Physical review X* **2012**. *2*, 011011.
- ⁴ Perera, A. From solutions to molecular emulsions. *Pure and Applied Chemistry* **2016**. *88*, 189.
- ⁵ Perera, A. Molecular emulsions: from charge order to domain order. *Phys. Chem. Chem. Phys.* **2017**. *19*, 28275–28285.
- ⁶ de Gennes, G., P. *Microscopic Structure and Dynamics of Liquids*. NATO Science Series B:. Springer New York, NY, 1 ed., **1977**.
- ⁷ Rowlinson, J. S.; Swinton, F. L. *Liquids and Liquid Mixtures*. Butterworths Monographs in Chemistry, **1982**.
- ⁸ Gennes, P. G. D.; Prost, J. *The Physics of Liquid Crystals*. Oxford University Press, **1993**.

- ⁹ Walker, J. S.; Vause, C. A. Lattice theory of binary fluid mixtures: Phase diagrams with upper and lower critical solution points from a renormalization-group calculation. *The Journal of Chemical Physics* **1983**. *79*, 2660.
- ¹⁰ Friedrich, L.; Požar, M.; Perera, A.; Paulus, M.; Thiering, N.; Savelkous, J.; Schneider, E.; Lovrinćević; Lützenkirchen-Hect, D.; Sternemann, C. Molecular micro-heterogeneity: Structure formation in amine-water mixtures. currently in review 2025.
- ¹¹ Požar, M.; Friedrich, L.; Lovrinćević, B.; Paulus, M.; Sternemann, C.; Perera, A. Microscopic structure of aqueous alkylamine mixtures: a computer simulation study. arXiv:2510.02146v1 2025.
- ¹² Teubner, M.; Strey, R. Origin of the scattering peak in microemulsions. The Journal of Chemical Physics 1987. 87, 3195.
- ¹³ Nelson, D.; Piran, T.; Weinberg, S. Statistical Mechanics of Membranes and Surfaces. World Scientific, 2nd ed., 2004.
- ¹⁴ Ma, S. Statistical Mechanics. World Scientific, 1985.
- ¹⁵ Berne, B. J.; Pecora, R. Dynamical Light Scattering with application to chemistry, biology and Physics. New-York: Wiley, 1976.
- ¹⁶ Cahn, J. W.; Hilliard, J. E. Free energy of a nonuniform system. i. interfacial free energy. *The Journal of Chemical Physics* 1958. 28, 258–267.
- ¹⁷ Hornreich, R. M.; Luban, M.; Shtrikman, S. Critical behavior at the onset of $\stackrel{\rightarrow}{k}$ -space instability on the λ line. *Phys. Rev. Lett.* **1975**. *35*, 1678–1681.
- ¹⁸ Debye, P. Zerstreuung von röntgenstrahlen. Annalen der Physik 1915. 351, 809–823.
- ¹⁹ Debye, P. Scattering of x-rays. In *The collected papers of Peter J.W. Debye*, Interscience Publishers. 1954.
- ²⁰ Požar, M.; Bolle, J.; Sternemann, C.; Perera, A. On the x-ray scattering pre-peak of linear mono-ols and the related microstructure from computer simulations. J. Phys. Chem. B 2020. 124, 8358–8371.
- ²¹ Ingólfsson, H. I.; Lopez, C. A.; Uusitalo, J. J.; de Jong, D. H.; Gopal, S. M.; Periole, X.; Marrink, S. J. The power of coarse graining in biomolecular simulations. WIREs Computational Molecular Science 2014. 4, 225–248.
- ²² Levitt, M. Birth and future of multiscale modeling for macromolecular systems (nobel lecture). *Angew Chem Int Ed Engl* **2014**. *53*, 10006–10018.
- ²³ Gray, C.; Gubbins, K. Theory of Molecular Fluids: I: Fundamentals. International Series of Monographs on Chemistry. OUP Oxford, 1984.

- ²⁴ Perera, A. Bridge function and fundamental measure theory: a test in dimension one. *Molecular Physics* 2009. 107, 2251–2259.
- ²⁵ Barrat, J.; Hansen, J.; Pastore, G. On the equilibrium structure of dense fluids. *Molecular Physics* 1988. 63, 747–767.
- ²⁶ Almásy, L.; Kuklin, A.; Požar, M.; Baptista, A.; Perera, A. Microscopic origin of the scattering pre-peak in aqueous propylamine mixtures: X-ray and neutron experiments versus simulations. *Phys. Chem. Chem. Phys.* **2019**. *21*, 9317–9325.
- ²⁷ Chew, P. Y.; Reinhardt, A. Phase diagrams—why they matter and how to predict them. *The Journal of Chemical Physics* **2023**. *158*, 030902.
- ²⁸ Perera, A.; Požar, M.; Lovrinčević, B. Camel back shaped kirkwood-buff integrals. The Journal of Chemical Physics 2022. 156, 124503.
- ²⁹ FISHER, M. E. Correlation functions and the critical region of simple fluids. Journal of Mathematical Physics 1964. 5, 944.
- ³⁰ Austin R. Saeger, W. G. C., J. Karl Johnson; Henderson, D. Cavity correlation and bridge functions at high density and near the critical point: a test of second-order percus—yevick theory. *Molecular Physics* 2016.
- ³¹ Llano-Restrepo, M.; Chapman, W. G. Bridge function and cavity correlation function for the lennard-jonesfrom simulation. *The Journal of Chemical Physics* 1992. 97, 2046.
- ³² Malijevský, A.; Labík, S. The bridge function for hard spheres. *Molecular Physics* 1987. 60, 663.
- ³³ Choudhury, N.; Ghosh, S. K. Integral equation theory of lennard-jones fluids: A modified verlet bridgefunction approach. *The Journal of Chemical Physics* 2002. 116, 8517.
- ³⁴ J. M. J. van Leeuwen, J. G.; de Boer, J. New method for the calculation of the pair correlation function. *Physica* 1959. 25, 792.
- ³⁵ Zerah, G.; Hansen, J. P. Self-consistent integral equations for fluid pair distribution functions: Another attempt. *The Journal of Chemical Physics* 1985. 84, 2336.
- ³⁶ Hirata, F. Molecular Theory of Fluctuation in Life Phenomena. Springer Nature Singapore, 2025.
- ³⁷ Fantoni, R.; Pastore, G. Computer simulation study of the closure relations in hard sphere fluids. *The Journal of Chemical Physics* **2004**. *120*, 10681.
- ³⁸ Cann, N. M. Improvement of integral equation theories for mixtures. The Journal of Chemical Physics 1999, 110, 11466.